Investigation of nanoscale structure in digital layers of Mn/GaAs and MnGa/GaAs

G. Kioseoglou, S. Kim, Y. L. Soo, X. Chen, H. Luo, and Y. H. Kao[a)]
Department of Physics, State University of New York at Buffalo, Buffalo, New York 14260

Y. Sasaki, X. Liu, and J. K. Furdyna
Department of Physics, University of Notre Dame, Notre Dame, Indiana 46556

(Received 4 October 2001; accepted for publication 4 December 2001)

Grazing incidence x-ray scattering (GIXS) and x-ray diffraction (XRD) techniques have been employed to study the microscopic structure of magnetic digital layers of Mn/GaAs and MnGa/GaAs. Samples with various GaAs layer thickness (8 to 16 monolayers) and a half monolayer of either Mn or MnGa were prepared by low-temperature molecular-beam epitaxy. All digital alloys consist of 50 periods of magnetic layers separated by GaAs. High crystalline quality was verified and the periodicity and layer thickness were determined from the GIXS and XRD data. In order to investigate the magnetic properties, we performed magnetization measurements on all samples using superconducting quantum interference device magnetometry (SQUID). © *2002 American Institute of Physics.* [DOI: 10.1063/1.1448658]

The possibility of spintronic applications with III–V diluted magnetic semiconductors such as $In_{1-x}Mn_xAs$ and $Ga_{1-x}Mn_xAs$ has generated significant interest in ferromagnetic semiconductors.[1–4] Because the new materials are III–V based alloys, spin-related effects could be integrated into established III–V semiconductor technology, making feasible the goal to fabricate a nonvolatile device. Ohno *et al.*[5,6] have succeeded in growing (Ga, Mn) As alloys by using low-temperature molecular-beam epitaxy (LT-MBE) to overcome the solubility limit of Mn in GaAs. The low-temperature growth was essential in suppressing the segregation of Mn and enabled higher Mn concentration samples to grow. Ferromagnetic order was observed in most of their samples with maximum Curie temperature $T_C \sim 110$ K for Mn concentrations between 4% and 5%. For Mn concentrations higher than 5%, the ferromagnetic order was suppressed and the T_C was reduced by more than half of its maximum value for Mn concentration >7%.

In this letter, we describe a study of the microscopic structure of magnetic digital layers of Mn/GaAs and MnGa/GaAs by using LT-MBE. This approach offers a better control over the position of the Mn atoms along the growth direction.[7] Because the structure combines the two types of materials in a digital alloy form, the carriers will interact with both constituents simultaneously. In other words, the material behaves as a ferromagnetic semiconductor for the carriers and it is believed that this type of digital alloys can then be used to inject spin-polarized carriers into nonmagnetic III–V structures. It is also expected that the similarity of such digital alloys and nonmagnetic III–Vs will greatly suppress the metal/semiconductor interface problem for vertical transport.[8]

The structural properties of these (Ga,Mn)As digital magnetic heterostructures are examined with grazing incidence x-ray scattering (GIXS) and x-ray Diffraction (XRD) techniques. GIXS is well suited for investigating layered structures. Structural parameters such as layer thickness, interfacial roughness, and correlation lengths can be determined with this technique. XRD on the other hand measures the lattice constant in layered structures, providing information on lattice distortion and strain.

We have studied two series of magnetic digital alloys of Mn/GaAs and MnGa/GaAs with their characteristics given in Table I. The main difference between the samples is the thickness of the GaAs layer sandwiched between the Mn (in the first series) and MnGa (in the second series) layers, ranging from 8 to 16 monolayers (ML). All samples were grown on (001) GaAs substrate. The growth follows the typical procedure for growing GaMnAs alloys, starting with an initial layer of 200 Å of GaAs at a substrate temperature of 580 °C to improve the GaAs surface for subsequent growth. The substrate temperature is then brought down to 275 °C and a low-temperature GaAs is grown to a thickness of a few hundred angstroms followed by the Mn/GaAs or the MnGa/GaAs digital alloy. The thickness of the Mn layers is estimated with reflection high-energy electron diffraction to be close to 0.5 ML while the MnGa layers consist of deposition sequence of Ga–Mn–Ga cycle. All digital layers consist of

TABLE I. Some characteristics of $[Mn/(GaAs)_n]_{50}/GaAs$ and $[MnGa/(GaAs)_n]_{50}/GaAs$ digital-layer samples used in this study. n = number of GaAs ML and T_s = substrate temperature in °C.

$[Mn/(GaAs)_n]_{50}$		
Sample	n (ML)	T_s
14A	8	275
14B	12	275
14D	16	275
$[MnGa/(GaAs)_n]_{50}$		
Sample	n (ML)	T_s
15D	8	275
15B	10	275
15C	16	275

a)Electronic mail: yhk@acsu.buffalo.edu

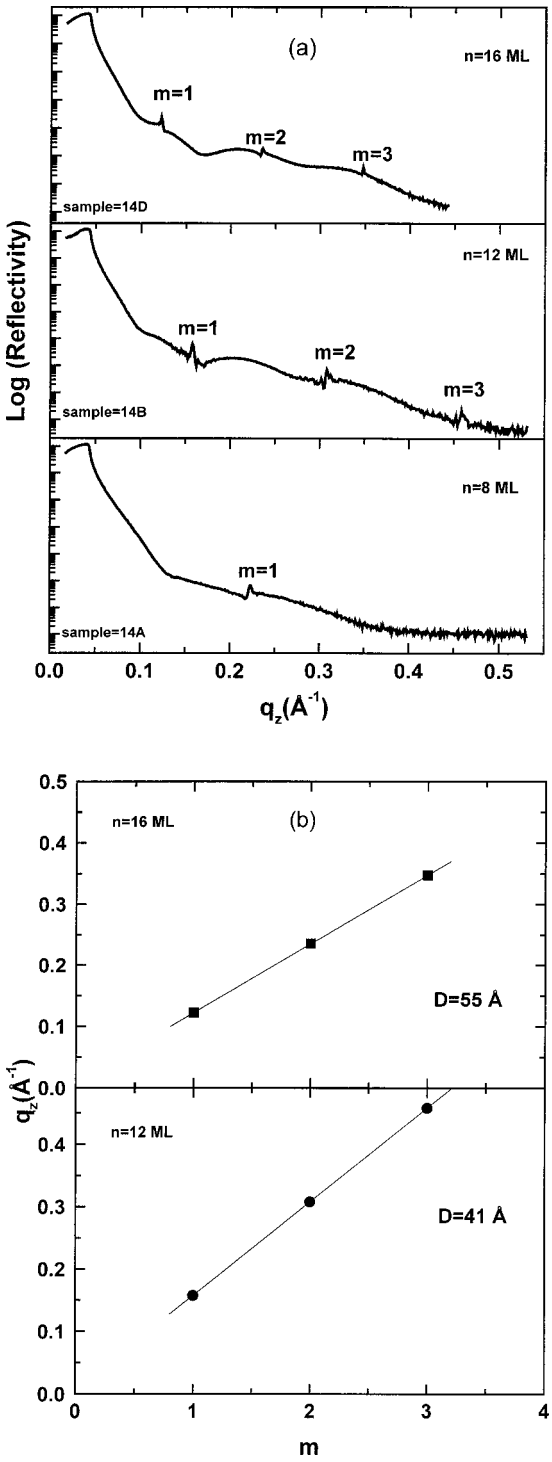

FIG. 1. (a) Grazing incidence x-ray scattering data for the samples 14A, 14B, and 14D of the $[\mathrm{Mn}/(\mathrm{GaAs})_n]_{50}$ series. (b) Determination of the period D of the digital alloy using the Bragg condition $q_z = 2\pi m/D$.

50 periods of such magnetic layers separated by GaAs.

The GIXS and XRD experiments were all carried out at beam line X3B1, at the National Synchrotron Light Source in Brookhaven National Laboratory. The energy of the incident x-ray beam was set at 10 keV. In Fig. 1(a), we plot the x-ray specular reflectivity for the three samples of the $[\mathrm{Mn}/(\mathrm{GaAs})_n]_{50}$ series as a function of q_z, the component of the scattering wave vector normal to the surface. We can clearly observe Bragg peaks associated with the artificially induced bilayer period D, up to the third order. In addition,

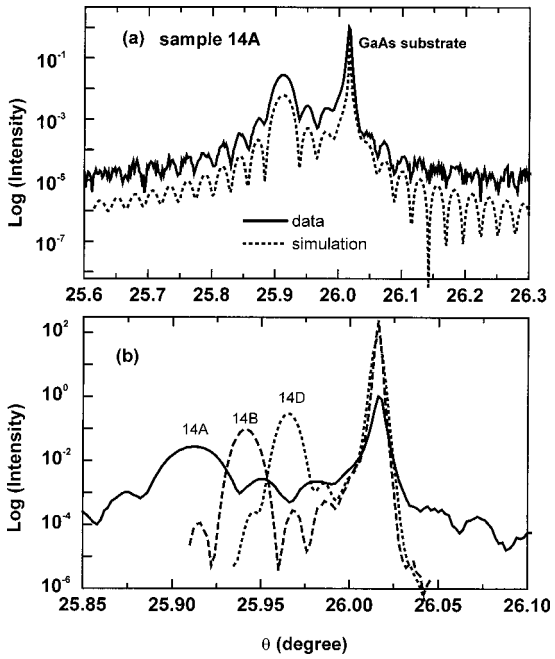

FIG. 2. (a) θ–2θ x-ray diffraction scan around GaAs (004) for sample 14A (8 ML). The dotted line is the simulated spectrum. (b) XRD around GaAs (004) for samples 14A, 14B, and 14D. Only a small portion of the spectra around the main peak is shown.

for the sample 14B ($n = 12$ ML) a number of small satellite peaks between the Bragg peaks is observed, resulting from the effect of the total thickness of the superlattice. These reflectivity results suggest that a superlattice structure was grown with sharp interfaces and well defined periodicity. By plotting q_z as function of the order m of the Bragg peaks [Fig. 1(b)] we can measure the period of the superlattice. The solid symbols in Fig. 1(b) are the measured peak positions and the solid line is a linear fit using the Bragg condition $q_z = 2\pi m/D$, where D is the period of the digital alloy. From the slope of this line, we obtain $D = 41$ Å for sample 14B ($n = 12$ ML) and $D = 55$ Å for sample 14D ($n = 16$ ML), which are close to the nominal values. For sample 14A ($n = 8$ ML) we observed only the first-order Bragg peak [Fig. 1(a)] which gives $D = 29$ Å.

Figure 2(a) shows a θ–2θ XRD scan around GaAs (004) for sample 14A with 8 ML of GaAs between the Mn layers. The main peak arising from the digital alloy appear at a lower angle with respect to that due to the GaAs substrate, implying an increase in the average lattice constant of the digital layer. The lattice constant determined from the position of the peak is $a = 5.6752$ Å, which is 0.39% greater than that of the GaAs. Fig. 2 also clearly shows the presence of Pendellösung fringes,[7,9] indicating that the two outer boundaries of the digital alloy are sharp and well defined. The dotted line in Fig. 2(a) is a simulation pattern around GaAs (004) for sample 14A and it was carried out using the value $D = 29$ Å for the period of the digital alloy determined from GIXS. The simulated spectrum which closely resembles the experimental data was obtained using 50 periods of Mn/GaAs layers and normal lattice spacing mismatch $\Delta a/a = 4.25 \times 10^{-3}$ (i.e., 0.425%). The positive value of $\Delta a/a$ implies that the digital layer is under compressive strain. It is interesting to mention that for the XRD simulation we have used the exact nominal value of 50 periods and the value

$D=29$ Å from GIXS; a close agreement between the results obtained with two different techniques also indicates a good crystalline structure throughout the digital alloy. In Fig. 2(b), we plot the x-ray diffraction around the GaAs (004) peak as a function of the incidence angle θ for the three samples 14A, 14B, and 14D in the $[\mathrm{Mn}/(\mathrm{GaAs})_n]_{50}$ series. Only a small portion of the spectrum is shown around the main peak of the digital layer. It can be seen that as the thickness of the GaAs layer between the Mn layers increases, the change in the lattice spacing mismatch of the digital layer in the normal direction decreases from 0.39% to 0.19%. XRD data of a superlattice often show satellite peaks around the main peak. We have only observed the zeroth-order peak while the absence of any satellite peak could most probably be due to thickness fluctuations within the 50 periods of the digital layer.

The reflectance data from the second series, $[\mathrm{MnGa}/(\mathrm{GaAs})_n]_{50}$ digital alloys, is similar to the ones presented for the first series. From the Bragg peaks, we were able to measure the period D of the digital alloy and obtain values close to the nominal.

In order to investigate the magnetic properties, we performed magnetization measurements on all the samples using SQUID magnetometry. Unlike MnGa epilayers that have a magnetization axis perpendicular to the MnGa layers, the easy axis for the digital-alloy samples is in the plane of the MnGa layers. The magnetization was studied as a function of temperature and an increase in Curie temperature (T_C) with wider GaAs spacers was observed. The highest T_C is found in sample 15C at approximately 60 K. It should be pointed out that these digital alloys are highly resistive, which should be taken into account in identifying the role of interlayer coupling. The magnetization of samples 14A, 14B, and 14D was also studied and it was found that while samples 14A (8 ML) and 14D (16 ML) are ferromagnetic, sample 14B (12 ML) shows paramagnetic behavior, which is presently not understood.

The x-ray results indicate that superlattice structures of excellent crystal quality were formed with abrupt interfaces between GaAs and either Mn or MnGa layers. The periodic thickness D calculated from the x-ray reflectivity results is in good agreement with the designed thickness, indicating excellent growth control. The reflectance data also indicate that diffusion of Mn into the neighboring GaAs layers should be very small. In other words, the Mn atoms most probably stay within the magnetic layers. This argument is supported also by the absence of the conduction band to Mn acceptor states transition (CB–A) from the photoluminescence (PL) spectra[10] taken at 10 K. In traditional alloys of GaMnAs where Mn ions are randomly distributed at Ga sites of the GaAs host, the Mn forms an acceptor center[11] and the CB–A transition dominates the PL spectra at energy ~ 1.41 eV. The absence of this CB–A transition from all the digital-layer structures used in this study implies the absence of isolated acceptor states in the GaAs layers and therefore a small percentage of Mn diffusion into the nonmagnetic layers.

Although GIXS and XRD techniques can be used to verify the periodic structure of the digital alloys and the high crystalline quality, these techniques do not address the following major questions: (i) the local environment of Mn ions in the digital-alloy structure and (ii) the Mn depth profile. To answer the first question, we have performed extended x-ray absorption fine structure and near-edge x-ray absorption fine structure (NEXAFS) experiments. The Mn valency obtained from the NEXAFS results is much less than two and closer to the metallic state, lending further support to our previous statement that Mn atoms most likely remain in the magnetic layers.[12] These results will be presented elsewhere.[13] The technique most appropriate to address the second question is the angular dependence of x-ray fluorescence. This method is element specific, nondestructive, and it can provide valuable information about the density profile of the Mn. Current efforts are aimed at quantifying the Mn depth profile.

In conclusion, we have used GIXS and XRD techniques to study the microscopic structure of magnetic digital layers of Mn/GaAs and MnGa/GaAs grown by LT-MBE. The reflectivity results suggest clearly that a superlattice structure was grown with sharp interfaces and very well defined periodicity (determined from the Bragg peaks). From the XRD spectra, we were able to measure the normal lattice spacing mismatch of the digital layer, while the presence of Pendellösung fringes indicates the sharpness of the two outer boundaries. The issue of diffusion of Mn into the neighboring GaAs layers was also discussed with reference to the PL and x-ray absorption fine structure measurements. Our results demonstrate that x-ray techniques are useful tools for probing nanoscale structures in the digital alloys, which are believed to play an important role in the development of a new spintronics technology.

The present research at SUNY-Buffalo is supported by the DOE and by DARPA under ONR Grant No. N00014-00-1-0951.

[1] H. Munekata, H. Ohno, S. von Molnar, A. Segmüller, L. L. Chang, and L. Esaki, Phys. Rev. Lett. **63**, 1849 (1989).
[2] H. Ohno, H. Munekata, T. Penney, S. von Molnar, and L. L. Chang, Phys. Rev. Lett. **68**, 2664 (1992).
[3] H. Ohno, A. Shen, F. Matsukura, A. Oiwa, A. Endo, S. Katsumoto, and Y. Iye, Appl. Phys. Lett. **69**, 363 (1996).
[4] H. Ohno, F. Matsukura, T. Omiya, and N. Akiba, J. Appl. Phys. **85**, 4277 (1999).
[5] A. Oiwa, S. Katsumoto, A. Endo, M. Hirasawa, Y. Iye, F. Matsukura, A. Shen, Y. Sugawara, and H. Ohno, Physica B **249**, 775 (1998).
[6] H. Ohno, Physica E (Amsterdam) **6**, 702 (2000).
[7] R. K. Kawakami, E. Johnston-Halperin, L. F. Chen, M. Hanson, N. Guébels, J. S. Speck, A. C. Gossard, and D. D. Awschalom, Appl. Phys. Lett. **77**, 2379 (2000).
[8] G. Schmidt and L. W. Molenkamp, Physica E (Amsterdam) **9**, 202 (2001).
[9] B. D. Cullity and S. R. Stock, *Elements of X-Ray Diffraction*, 3rd ed. (Prentice–Hall, Englewood Cliffs, New Jersey, 2001).
[10] M. Furis, X. Chen, H. Luo, A. Petrou, Y. Sasaki, X. Liu, and J. K. Furdyna (unpublished).
[11] J. Szczytko, A. Twardowski, K. Światek, M. Palczewska, M. Tanaka, T. Hayashi, and K. Ando, Phys. Rev. B **60**, 8304 (1999).
[12] It is possible that the formation of Mn cluster will give rise to an antiferromagnetic Mn–Mn interaction which reduces the valency to a value much lower than 2.
[13] Y. L. Soo, G. Kioseoglou, S. Kim, X. Chen, H. Luo, Y. H. Kao, Y. Sasaki, X. Liu, and J. K. Furdyna (unpublished).